POSITION AND ORIENTATION CONTROL OF A STEWART PLATFORM HYDRAULICALLY DRIVEN BY PRESSURE CONTROL SERVOVALVES

Marcio Aurelio Furtado Montezuma
Centro Federal de Educação Tecnológica do Paraná – Cornélio Procópio, montezum@sc.usp.br

Alexandre Simião Caporali
Escola de Engenharia de São Carlos – Universidade de São Paulo, caporali@usp.br

Eduardo Morgado Belo
Escola de Engenharia de São Carlos – Universidade de São Paulo, belo@sc.usp.br

Abstract. This work shows the position and orientation control of a non-linear model of a Stewart platform with six degrees of freedom developed in the multibody systems environment *ADAMS®* (*MSC.Software Corporation*). The non-linear model is exported to *SIMULINK®* (*MathWorks, Inc.*), where the position and orientation control system is implemented as a tracking one with state-feedback using the corresponding previously designed linear model controller. The *SIMULINK®* is also used to implement the dynamics of the servovalves and hydraulic cylinders with pressure control servovalves and to simulate the dynamic behavior of the flight simulator with hydraulic drives. These commercial packages are used seeking to save time and effort in the modeling of complex mechanical systems and in the programming to get the time response of the system, facilitating the analysis of several Stewart platforms configurations.

Keywords: multivariable control; Stewart platform; tracking systems; hydraulic systems; servovalve.

1. INTRODUCTION

Closed-kinematic chain manipulators that comprise two platforms coupled together by six linear parallel actuators whose length variations produce the motion of one platform relative to another are classified as Stewart platform-based manipulators. The development of the above mechanism proposed by Stewart (1965/66) in the design of an aircraft simulator was motivated by disadvantages suffered by conventional anthropomorphic open-kinematic chain manipulators whose joints and links are actuated in series (Nguyen et al., 1993).

If the length of pistons change, an end-effector attached to the mobile platform can be moved in six degrees of freedom space to obtain desired configuration (position and orientation) (Geng et al., 1992). They have higher structural strength and higher stiffness since the load is proportionally distributed by all six actuators. They can achieve higher accuracy in positioning and motion because the positioning error on each actuator is averaged out instead of being accumulated at the end-effector (Geng et al., 1992 and Lebret et al., 1993).

In general, there is a duality between parallel robots and serial linkage robots. For a 6-dof Stewart platform, the complexity of the forward kinematics has to be compared with that of the direct kinematics of the serial robot and, on the contrary, inverse kinematics are as easy as the forward kinematics of serial robot arm (Geng et al., 1992 and Lebret et al., 1993).

Many variants of this structure have since been investigated; most of them are configurations having six linearly actuated links with different combinations of link-platform connections such as 3-3, 3-6, and the more general 6-6 (Fig. 1) (Ben-Horin et al., 1998).

Figure 1 - Stewart platform configurations.

We used a Stewart platform with configuration 3-3, with two equal triangular platforms. The actuators are connected to the movable platform by spherical joints and to the stationary platform by universal joints. This configuration is known as cubical Stewart platform because the actuators are positioned as cubic edge.

Although much of the research in the literature has devoted extensive effort to the kinematics, dynamics and mechanism design of Stewart platform-based manipulators, little attention has been paid to the control problem of this type of manipulators (Nguyen et al., 1993).

The goal is to apply a position and orientation control to the movable platform with respect to the stationary platform.

2. INVERSE KINEMATICS

Manipulation tasks are usually given as a set of position and orientation with respect to the global coordinate frame of the robot's end-effector trajectory. To achieve these tasks is necessary to transform end-effector trajectory into active joints motion. This transformation also known as the inverse kinematics problem is, in our case, the calculation of the position of the six actuators from a given position and orientation of the movable platform (Ben-Horin et al., 1998).

To define the Cartesian variables we proceed to assign two coordinate frames {A} and {B} where the first is local coordinate system that is chosen to be the centroid of the stationary platform and the second is global coordinate system of the movable platform and has its origin at the mass center (Fig. 2).

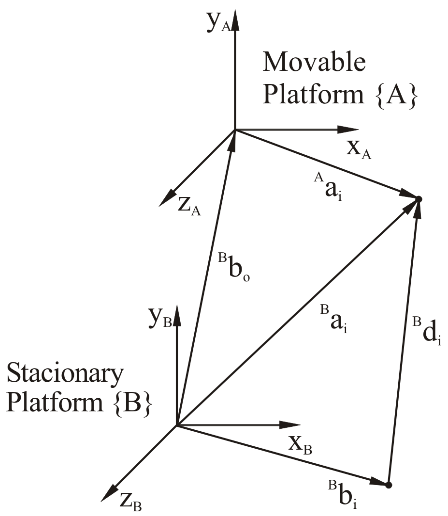

Figure 2 – Vector diagram for the *i*th actuator.

If ${}^{B}\boldsymbol{b_i} = (b_{ix}\ b_{iy}\ b_{iz})^T$ describe the position of the attachment of the universal joint in the stationary platform with respect to the coordinate system {B}; ${}^{A}\boldsymbol{a_i} = (a_{ix}\ a_{iy}\ a_{iz})^T$ is the position of the attachment of the spherical joint to the movable platform with respect to the coordinate system {A} and ${}^{B}\boldsymbol{b_o} = (x\ y\ z)$ is the position of the origin of {A} with respect to {B}, then we can say that

$$ {}^{B}\boldsymbol{a_i} = {}^{B}\boldsymbol{b_o} + {}^{B}_{A}\boldsymbol{R}\ {}^{A}\boldsymbol{a}_i \tag{1} $$

where ${}^{B}_{A}\boldsymbol{R}$ is the orientation matrix.

The length of the actuator given by the norm of the vector ${}^{B}\boldsymbol{d_i} = (d_{ix}\ d_{iy}\ d_{iz})^T$ with respect to the global coordinate system can be computed by

$$ {}^{B}\boldsymbol{d_i} = {}^{B}\boldsymbol{a_i} - {}^{B}\boldsymbol{b_i} \tag{2} $$

There are several ways to represent an orientation by three variables. But the most widely used one is the Euler Angles Z-Y-X (Nguyen and Pooran, 1989), which represent the orientation of coordinate system {A}, obtained after the following sequence of rotations from coordinate system {B}:

- A rotation of an angle α about the axis z_B.
- A rotation of an angle β about the new axis y'_B.
- A rotation of an angle γ about the new axis x''_B.

The orientation represented by α, β and γ is given by

$$ \boldsymbol{R}_{zyx}(\alpha,\beta,\gamma) = \begin{bmatrix} c\alpha c\beta & c\alpha s\beta s\gamma - s\alpha c\gamma & c\alpha s\beta c\gamma + s\alpha s\gamma \\ s\alpha c\beta & s\alpha s\beta s\gamma + c\alpha c\gamma & s\alpha s\beta c\gamma - c\alpha s\gamma \\ -s\beta & c\beta s\gamma & c\beta c\gamma \end{bmatrix} = {}^{B}_{A}\boldsymbol{R} \ \therefore\ c = \cos()\ e\ s = sen(). \tag{3} $$

Substituting Eq. (1) into Eq. (2), we obtain

$$ {}^{B}\boldsymbol{d_i} = {}^{B}_{A}\boldsymbol{R}\ {}^{A}\boldsymbol{a_i} + {}^{B}\boldsymbol{b_o} - {}^{B}\boldsymbol{b_i} \quad \textit{for } i = 1,2,\ldots 6, \tag{4} $$

furthermore, the length of the vector ${}^{B}\boldsymbol{d_i}$, called l_i can be computed from the vector components as

$$ l_i = (d_{ix}{}^2 + d_{iy}{}^2 + d_{iz}{}^2)^{1/2} \tag{5} $$

Equation (5) can be rewritten, applying Eq. (4) and the properties about orthonormal orientation matrix, as

$$ \begin{aligned} l_i^2 &= x^2 + y^2 + z^2 + a_{ix}^2 + a_{iy}^2 + a_{iz}^2 \\ &\quad + b_{ix}^2 + b_{iy}^2 + b_{iz}^2 + \\ &\quad + 2(r_{11}\,a_{ix} + r_{12}\,a_{iy} + r_{13}\,a_{iz})(x - b_{ix}) \\ &\quad + 2(r_{21}\,a_{ix} + r_{22}\,a_{iy} + r_{23}\,a_{iz})(y - b_{iy}) \\ &\quad + 2(r_{31}\,a_{ix} + r_{32}\,a_{iy} + r_{33}\,a_{iz})(z - b_{iz}) \\ &\quad - 2(xb_{ix} + yb_{iy} + zb_{iz}) \\ &\textit{for } i = 1,2,\ldots 6. \end{aligned} \tag{6} $$

Then given the position ${}^{B}\boldsymbol{b_o} = (x\ y\ z)^T$ and an orientation $(\alpha\ \beta\ \gamma)$, we can determine the length l_i of the actuators that lead the movable platform to the desired configuration.

3. STEWART PLATFORM DYNAMICS

If compared with the wide literature about Stewart platform kinematics, the studies of dynamics are relatively few (Dasgupta and Mruthyunjaya, 2000). Important contributions can be found in Fichter (1986) and Merlet (1987), which are applicable if the inertia of the actuators and the friction on joints have been despised. Besides there are other works as Nguyen and Pooran (1989), Geng et al. (1992), Liu et al. (1993) and Ji (1994). Herewith we can note the level of difficulty to get the model that represents dynamic behavior of the platform.

We used two Stewart platform models obtained from dynamic modeling software *ADAMS*®. One is linear and other is non-linear model both contained six inputs that are actuators forces and twelve outputs, where six are the actuators displacements and the other six are differentials of these displacements.

The linear model in state-space has been used to do the control about the linearization point. It is constituted by four matrixes: $\boldsymbol{A}$, $\boldsymbol{B}$, $\boldsymbol{C}$ and $\boldsymbol{D}$. The $\boldsymbol{A}$ is a $n \times n$ matrix where n is a number of states being equal to two times the number of system degree of freedom. As Stewart platform has six degrees of freedom this is equal to twelve. The $\boldsymbol{B}$ is $n \times m$ matrix where m is six that is the number of system inputs. The $\boldsymbol{C}$ is $p \times n$ where p is the number of system outputs and $\boldsymbol{D}$ is $p \times m$ with all its null elements.

The non-linear model has been used to simulate the real platform behavior and to test the control performance (Fig. 3).

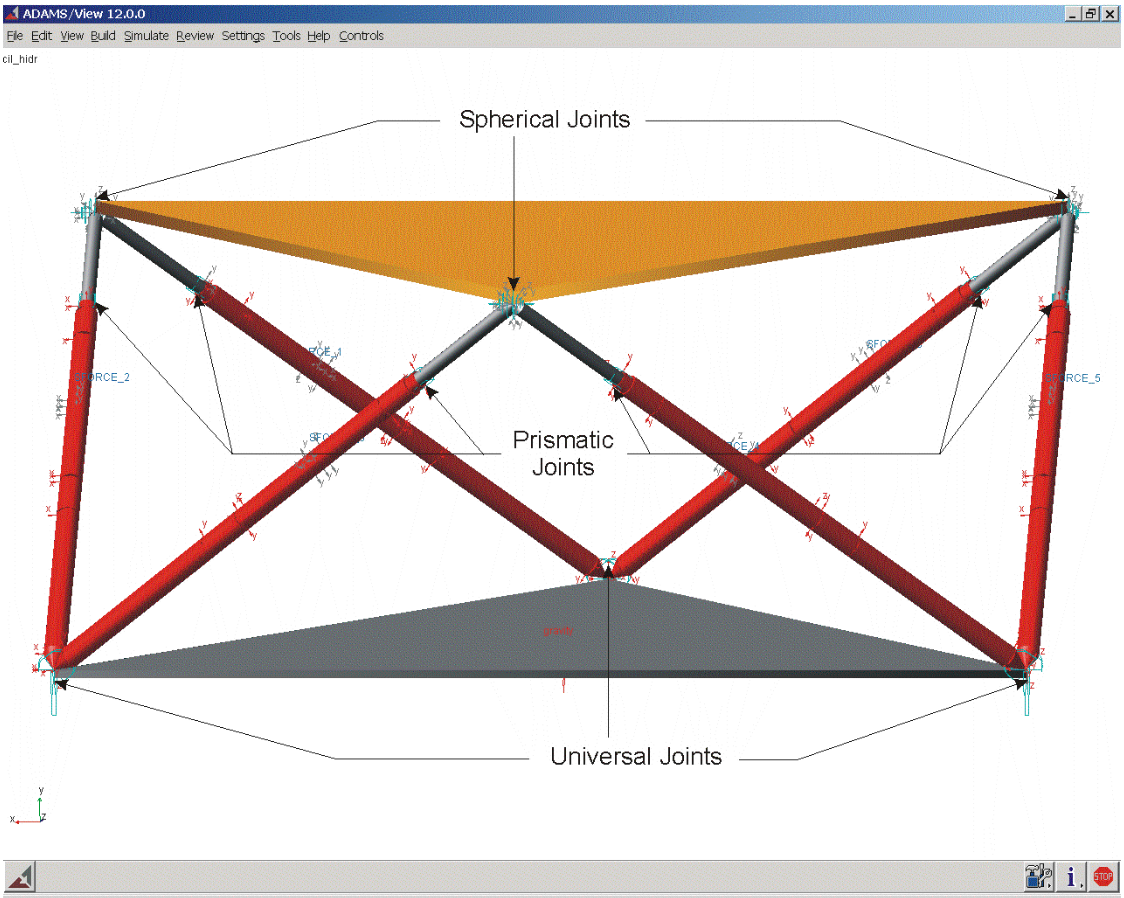

Figure 3 – Stewart platform modeling in *ADAMS*®.

4. CONTROL SYSTEM

A controllable open-loop system is represented by the nth-order state and pth-order output equations of the form

$$\dot{\boldsymbol{x}} = \boldsymbol{A}\boldsymbol{x} + \boldsymbol{B}\boldsymbol{u} \tag{7}$$

$$\boldsymbol{y} = \boldsymbol{C}\boldsymbol{x} = \begin{bmatrix} \boldsymbol{E} \\ \boldsymbol{F} \end{bmatrix} \boldsymbol{x} \tag{8}$$

where $\boldsymbol{y}$ is a vector $p \times 1$ and $\boldsymbol{w} = \boldsymbol{E}\boldsymbol{x}$ is a vector $m \times 1$ representing the outputs that are required to follow an input vector $\boldsymbol{r}$.

The control design method consists of the addition of a vector comparator and integrator that satisfies the equation (D'Azzo and Houpis, 1995)

$$\dot{\boldsymbol{z}} = \boldsymbol{r} - \boldsymbol{w} = \boldsymbol{r} - \boldsymbol{E}\boldsymbol{x} . \tag{9}$$

The state-feedback control law to be used is

$$\boldsymbol{u} = \boldsymbol{K}_1\boldsymbol{x} + \boldsymbol{K}_2\boldsymbol{z} = \begin{bmatrix} \boldsymbol{K}_1 & \boldsymbol{K}_2 \end{bmatrix} \begin{bmatrix} \boldsymbol{x} \\ \boldsymbol{z} \end{bmatrix} \tag{10}$$

$$\overline{\boldsymbol{K}} = \begin{bmatrix} \boldsymbol{K}_1 & \boldsymbol{K}_2 \end{bmatrix}. \tag{11}$$

This control law assigns the desired closed-loop eigenvalue spectrum if and only if $(\boldsymbol{A},\boldsymbol{B})$ is a controllable pair, and

$$rank \begin{bmatrix} \boldsymbol{B} & \boldsymbol{A} \\ \boldsymbol{0} & -\boldsymbol{E} \end{bmatrix} = n + m . \tag{12}$$

Equation (12) can be satisfied only if the number of $\boldsymbol{w}(t)$ outputs that are required to track the input $\boldsymbol{r}(t)$ is less than or equal to the number of control input m.

Satisfaction of the condition of Eq. (12) guarantees that a control law of the form of Eq. (10) can be synthesized so that the closed-loop outputs tracks the command input (D'Azzo and Houpis, 1995). In that case the closed-loop state and output equations are

$$\dot{\boldsymbol{x}}' = \begin{bmatrix} \dot{\boldsymbol{x}} \\ \dot{\boldsymbol{z}} \end{bmatrix} = \begin{bmatrix} \boldsymbol{A} + \boldsymbol{B}\boldsymbol{K}_1 & \boldsymbol{B}\boldsymbol{K}_2 \\ -\boldsymbol{E} & \boldsymbol{0} \end{bmatrix} \begin{bmatrix} \boldsymbol{x} \\ \boldsymbol{z} \end{bmatrix} + \begin{bmatrix} \boldsymbol{0} \\ \boldsymbol{I} \end{bmatrix} \boldsymbol{r} = \boldsymbol{A}'_{cl}\boldsymbol{x}' + \boldsymbol{B}'\boldsymbol{r} \tag{13}$$

$$\boldsymbol{y} = \begin{bmatrix} \boldsymbol{C} & \boldsymbol{0} \end{bmatrix} \begin{bmatrix} \boldsymbol{x} \\ \boldsymbol{z} \end{bmatrix} = \overline{\boldsymbol{C}}\boldsymbol{x}' . \tag{14}$$

The feedback matrix of Eq. (11) can be selected so that the eigenvalues are in the left-half plane for the closed-loop plant matrix of Eq. (13). Thus, the outputs $\boldsymbol{w}(t)$ track the piecewise constant command vector $\boldsymbol{r}(t)$ in the steady state. The control system is illustrated in Fig. (4).

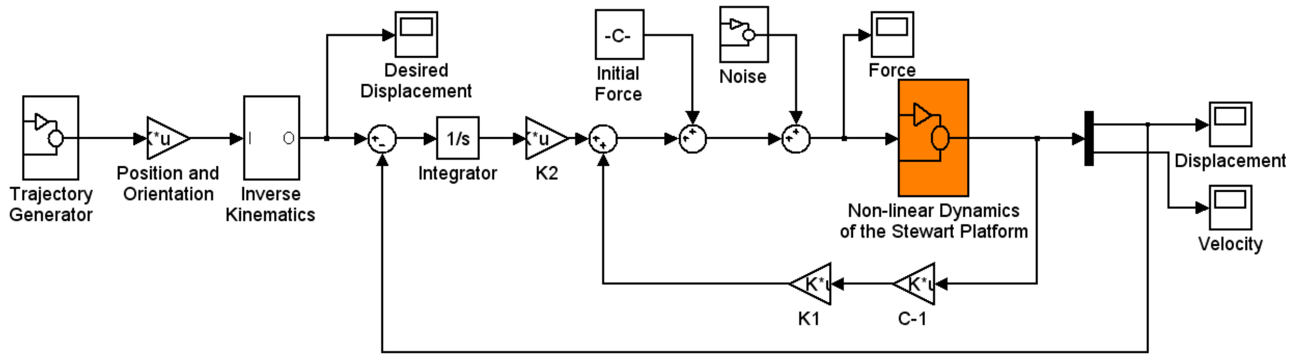

Figure 4 – Tracking system.

5. HYDRAULIC SYSTEM DYNAMICS IMPLEMENTATION

Due to the hydraulic system modeling hasn't been considered to get the matrixes $\boldsymbol{K_1}$ and $\boldsymbol{K_2}$ of the tracking control system, the inclusion of the hydraulic system must be done so that it doesn't change the control system and Stewart platform closed-loop equations. It was used, then, a servovalve with a pressure-control servo that is one control system which measures its own output and forces the output to quickly and accurately follow a command signal. Both actuators force determined by control system with state-feedback and the actuators crown area are used to get the desired load pressure P_L to each actuator. These is the command signal that must be compared with the pressure difference between the actuators lines measured with a transducing device to convert it to an electrical signal. This feedback signal is compared with the command signal, and the resulting error signal is then amplified through the controller and used to drive the servovalve (Neal, 1974).

The system output load pressure P_L is subtracted from reference pressure P_{Lref} producing an error that will be the PI (proportional-integral) control input. The control system output, i.e., the servovalve control action u is an electrical signal proportional to servovalve spool displacement x_v. The servo *SIMULINK®* blocks diagram is illustrated in Fig. (5).

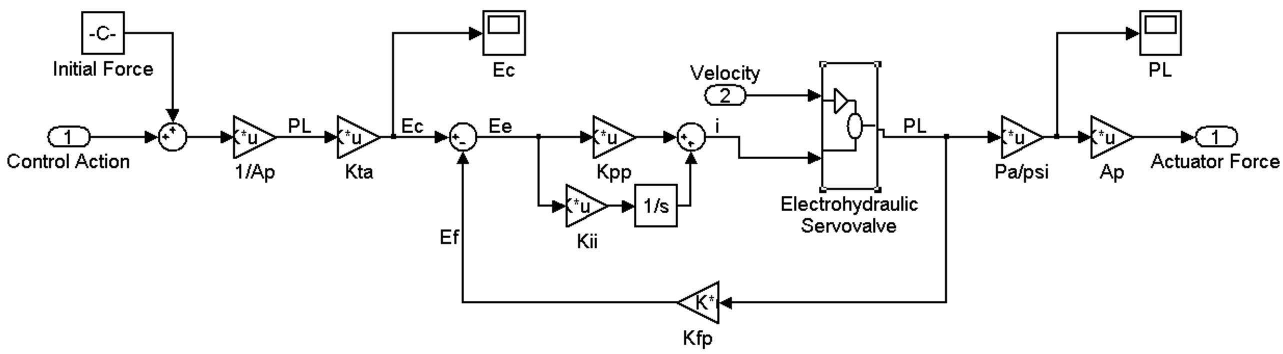

Figure 5 – Pressure-control servo blocks diagram.

To represent the servovalve was used a model in which the torque motor, the flapper-nozzle and the hydraulic amplifier behavior are considered in modeling. This model was developed to pressure control servovalve 15-010 made by *Moog Inc*. (Fig. 6).

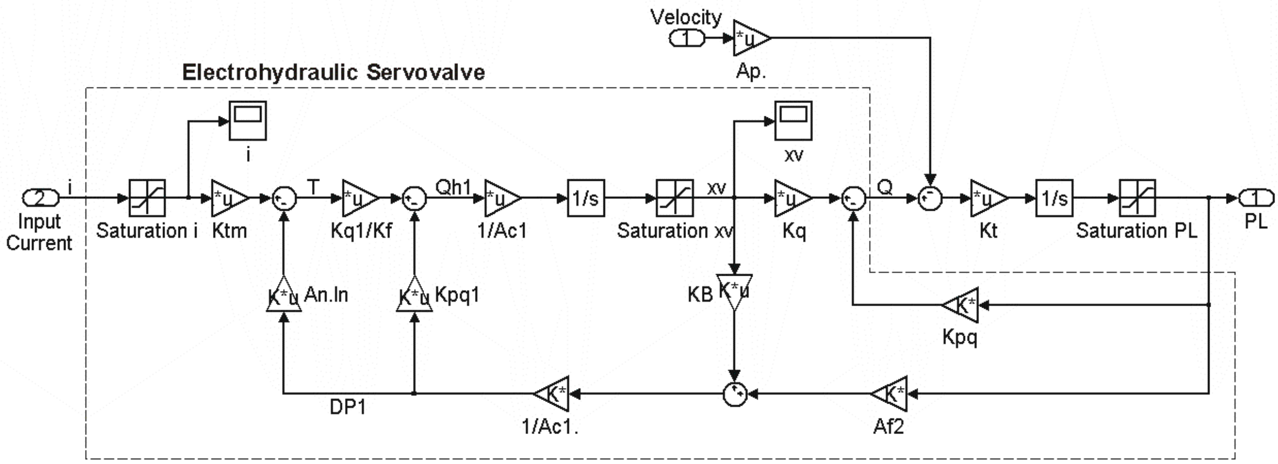

Figure 6 – Pressure control servovalve blocks diagram (Moog, 2002).

The flow gain, flow-pressure and total leakage coefficients were estimated from the fabricant catalog of the servovalve. The other values were computed or estimated from both literature and fabricant catalog indication.

The parameters values used in the simulation can be obtained in Montezuma (2003).

6. SIMULATION RESULTS

We have used simulation to check if the control obtained from the linear model can control the non-linear model appropriately around the linearization point.

To avoid movements by gravity action before the control actuates to establish the position, we use an initial value to the action control that maintains the Stewart platform in the initial position (Fig. 4).

To test the control was used a ramp input

$$\delta(t) = \begin{cases} 0, \; para \;\; 0 \le t < 1 \\ t-1, \; para \;\; 1 \le t < 2 \\ 1, \; para \;\; t \ge 2 \end{cases} \tag{15}$$

that multiply the position and orientation vector $(x \;\; y \;\; z \;\; \alpha \;\; \beta \;\; \gamma)^T$. Its values are

$$\begin{aligned} & x = 0 \; mm; y = 30 \; mm; z = 0 \; mm \\ & \alpha = \pi / 60; \beta = \pi / 60; \gamma = \pi / 18 \end{aligned} \tag{16}$$

that results in the following displacements of the linear actuator calculated through the inverse kinematics

$$\begin{aligned} \boldsymbol{r} &= [l_1 \;\; l_2 \;\; \dots \;\; l_6]^T \\ &= [46.4425 \quad -77.1581 \quad 215.1399 \\ &\quad 107.0298 \;\; -39.9325 \;\; -137.5990]^T. \end{aligned} \tag{17}$$

The feedback controller is required to cause the output vector $\boldsymbol{w}$ to track the command input $\boldsymbol{r}$ in the steady state.

The simulations were done taking into account the complete system with the pressure-control servo and the hydraulic system dynamics (Fig. 7).

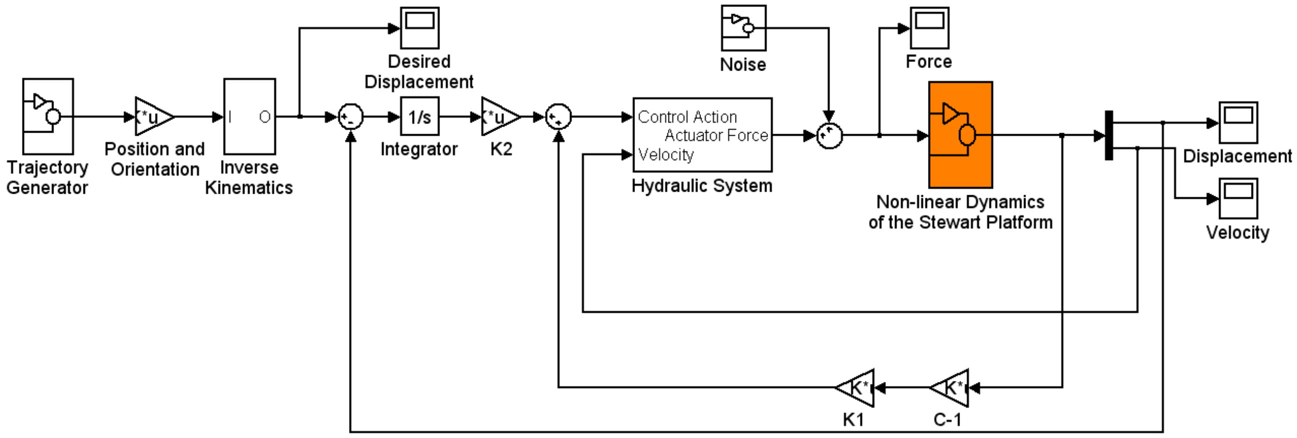

Figure 7 – Tracking system with the pressure-control servo and the hydraulic system dynamics.

We can observe through the actuators displacement graphic (Fig. 8) that the output vector $\boldsymbol{w}$ is equal to the command input $\boldsymbol{r}$ in the steady state, as required. The actuators velocity and force graphic are used to determine the drive system characteristics as pressure and flow of the bomb in the hydraulic systems or power and rotation in the electric systems (Fig. 8).

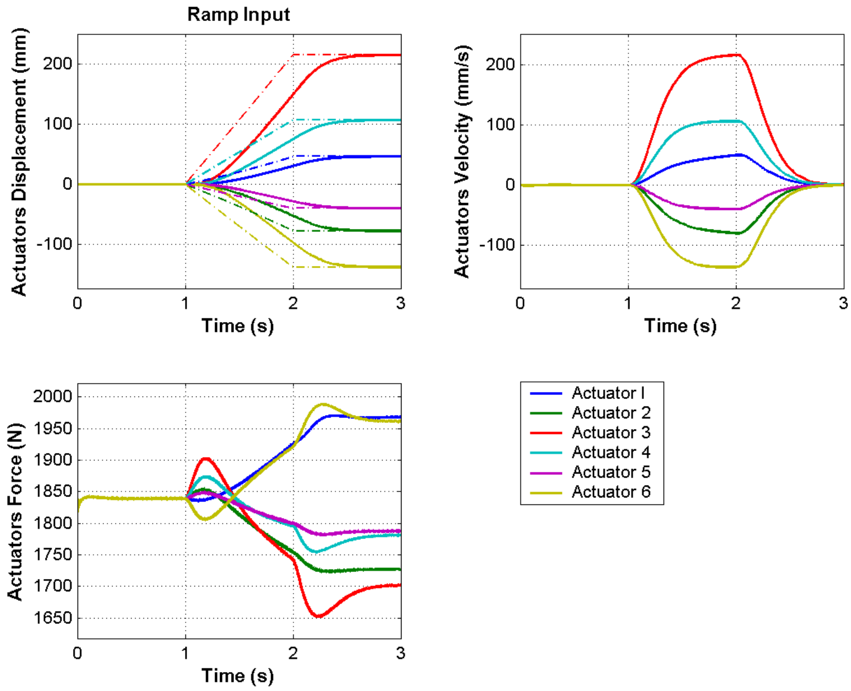

Figure 8 – Actuators displacement, velocity and force.

Looking at the hydraulic system parameters graphic we can observe that there is a noise in the input current response which can be caused by a numeric problem (Fig. 9).

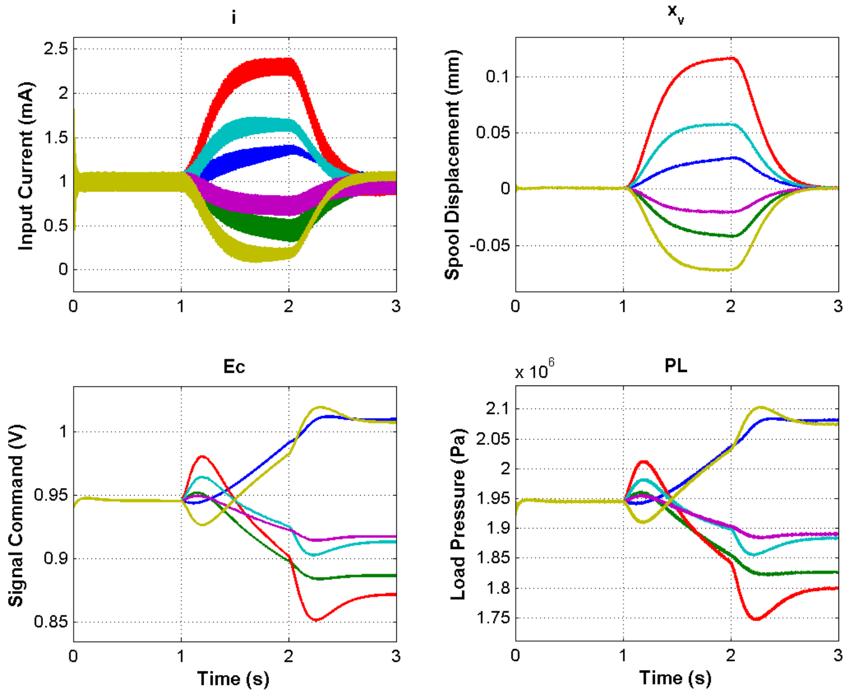

Figure 9 – Hydraulic system and pressure-control servo parameters.

The eigenvalues assigned to the system must be such that Stewart platform responds faster than the system which is desired to simulate as an airplane, a robot or a milling machine. In the case of an airplane the fastest mode, the short period, is around the 4.0 Hz for acrobatic airplanes to the 0.1 Hz for large commercial airplanes (McLean, 1990). Otherwise, the elements of the gain matrix $\overline{\boldsymbol{K}}$ mustn't have high values that impede the physical implementation of the system, both with respect to the noise amplification and the necessity of high energy that is limited by characteristics of the actuator systems. Based in these questions, we define the following eigenvalues set to the closed-loop plant $\boldsymbol{A}'_{cl}$

$$\sigma\left(\overline{\boldsymbol{A}}+\overline{\boldsymbol{B}}\overline{\boldsymbol{K}}\right)=\left\{\underbrace{-9,\ldots-9}_{6\ eigenvalues},\underbrace{-10,\ldots-10}_{6\ eigenvalues},\underbrace{-11,\ldots-11}_{6\ eigenvalues}\right\}\therefore \qquad (18)$$

$$9\ rad/s=1{,}43\ Hz,\ 10\ rad/s=1{,}59\ Hz,\ 11\ rad/s=1{,}75\ Hz$$

that satisfies the conditions previously established to commercial airplanes.

7. CONCLUSIONS

The utilization of the commercial package of the dynamic modeling *ADAMS®* was very important to give flexibility and quickness to obtain a complex dynamic model. The tracking system used is efficient to control the position and orientation of the Stewart platform non-linear model, even to large displacements. One difficulty found was the fact of the linearization done by *ADAMS®* to result in a matrix system, so that multiplication of $\boldsymbol{C}$ by $\boldsymbol{B}$, known as Markov parameter, that has a null rank. This makes impossible the utilization of some multivariable control techniques as tracking systems using output feedback.

The model of hydraulic system and pressure-control servo used show to be efficient to the simulations that were done, it being able to be simulated quickly with consistent results.

Although this modeling and simulation process has been applied to the Stewart platform with the purpose of studying the flight simulator behavior, the method can be used to model and simulate other kind of systems as active suspension, automatic pilot of car, robot, robotic gripe, etc. The goal of this work is to test and define a methodology to modeling and simulation of complex systems with many degrees of freedom in a quick and efficient way.

8. REFERENCE

Ben-Horin, R., Shoham, M., and Djerassi, S. (1998). Kinematics, Dynamics and Constrution Planarly Actuated Parallel Robot. In: *Robotics Computer-Integrated Manufacturing*, v. 14, p. 163-172.

Dasgupta, B. and Mruthyunjaya, T.S. (2000). The Stewart Platform Manipulator: a Review. *Mechanism and Machine Theory*, v. 35, p. 15-40.

D'Azzo, J. J. and Houpis, H.C. (1995). *Linear Control System Analysis and Desing: Conventional and Modern*. 4th ed., New York, McGraw Hill, Inc.

Fichter, E.F. (1986). A Stewart Platform-Based Manipulator: General Theory and Pratical Construction. *The International Journal of Robotics Research,* v. 5, n. 2, p. 157-182.

Geng, Z. et al. (1992). On the Dynamic Model and Kinematic Analysis of a Class of Stewart Platforms. *Robotics and Autonomous Systems*, v. 9, p. 237-254.

Ji, Z. (1994). Dynamic Decomposition for Stewart Platforms. *ASME Journal of Mechanical Design*, v. 116, n. 1, p. 67-69. March.

Lebret, G., Liu, K. and Lewis, F.L. (1993). Dynamic Analysis and Control of a Stewart Platform Manipulator. *Journal of Robotic System*, v. 10, n. 5, p. 629-655.

Liu, K. et al. (1993). The Singularities and Dynamics of a Stewart Platform Manipulator. *Journal of Intelligent and Robotic Systems*, v. 8, p. 287-308.

McLean, D. (1990). *Automatic Flight Control Systems*. New York, Prentice Hall International Ltd.

Merlet, J.-P. (1987). Parallel Manipulator, Part I, Theory. *INRIA Research Report nº 646.*

Moog (2002). *15 series servovalve*. Available in: <www.moog.com/noq/_general_c339>. Access in: Dec 5.

Montezuma, M.A.F. (2003). *Modelagem e controle de posição e orientação de uma plataforma de Stewart*. São Carlos, 2003. 124p. Dissertação (Mestrado) – Escola de Engenharia de São Carlos, Universidade de São Paulo.

Neal, T.P. (1974). *Performance estimation for electrohydraulic control systems*. Moog Inc. Controls Division, East Aurora, New York. (Techinical Bulletin 126).

Nguyen, C.C. and Pooran, F.J. (1989). Dynamic Analysis of a 6 DOF CKCM Robot End-effector for Dual-arm Telerobot Systems. *Robotics and Autonomous Systems*, v. 5, p. 377-394.

Nguyen, C.C. et al. (1993). Adaptive Control of a Stewart Platform-Based Manipulator. *Journal of Robotic Systems*, v. 10, n. 5, p. 657-687.

Stewart, D. (1965/66). A Platform with Six Degrees of Freedom. *Proc. Instituite of Mechanical Engineering*, part I, v.180, n. 5, p. 371-386.